Published in final edited form as:
Curr Neurovasc Res. 2012 February 1; 9(1): 20–31.

Wnt1 Inducible Signaling Pathway Protein 1 (WISP1) Blocks Neurodegeneration through Phosphoinositide 3 Kinase/Akt1 and Apoptotic Mitochondrial Signaling Involving Bad, Bax, Bim, and Bcl-x_L

Shaohui Wang[1,2,3], **Zhao Zhong Chong**[1,2,3], **Yan Chen Shang**[1,2,3], and **Kenneth Maiese**[*,1,2,3]

[1]Laboratory of Cellular and Molecular Signaling, University of Medicine and Dentistry, New Jersey Medical School, Newark, 07101 New Jersey, USA

[2]Department of Neurology and Neurosciences, University of Medicine and Dentistry, New Jersey Medical School, Newark, 07101 New Jersey, USA

[3]Cancer Center, New Jersey Medical School, University of Medicine and Dentistry, New Jersey Medical School, Newark, 07101 New Jersey, USA

Abstract

Wnt1 inducible signaling pathway protein 1 (WISP1) is a member of the CCN family of proteins that determine cell growth, cell differentiation, immune system activation, and cell survival in tissues ranging from the cardiovascular-pulmonary system to the reproductive system. Yet, little is known of the role of WISP1 as a neuroprotective entity in the nervous system. Here we demonstrate that WISP1 is present in primary hippocampal neurons during oxidant stress with oxygen-glucose deprivation (OGD). WISP1 expression is significantly enhanced during OGD exposure by the cysteine-rich glycosylated protein Wnt1. Similar to the neuroprotective capabilities known for Wnt1 and its signaling pathways, WISP1 averts neuronal cell injury and apoptotic degeneration during oxidative stress exposure. WISP1 requires activation of phosphoinositide 3-kinase (PI 3-K) and Akt1 pathways to promote neuronal cell survival, since blockade of these pathways abrogates cellular protection. Furthermore, WISP1 through PI 3-K and Akt1 phosphorylates Bad and GSK-3β, minimizes expression of the Bim/Bax complex while increasing the expression of Bcl-x_L/Bax complex, and prevents mitochondrial membrane permeability, cytochrome c release, and caspase 3 activation in the presence of oxidant stress. These studies provide novel considerations for the development of WISP1 as an effective and robust therapeutic target not only for neurodegenerative disorders, but also for disease entities throughout the body.

Keywords

Akt1; apoptosis; Bax; Bcl-x_L; Bim; brain; cytochrome c; GSK-3β; mitochondria; nervous system; PI 3-K; WISP; Wnt1; oxidative stress

[*]Address correspondence to this author at the Department of Neurology and Neurosciences, Cancer Center, F 1220, UMDNJ – New Jersey Medical School, 205 South Orange Avenue, Newark, NJ 07101, USA; wntin75@yahoo.com.

DISCLOSURES

The authors have nothing to disclose.

INTRODUCTION

Wnt1 inducible signaling pathway protein 1 (WISP1) is a cysteine rich secreted matricellular protein. WISP1 is a member of the CCN family of proteins that is defined by the first three members of the family that include Cysteine-rich protein 61, Connective tissue growth factor, and Nephroblastoma overexpressed gene [1]. The CCN family of proteins play important roles in cell growth, differentiation, immune modulation, and cell survival [1–3]. WISP1 was identified as a downstream target of Wnt1 signaling pathway in the mouse mammary epithelial cell line C57MG transformed by Wnt1 [4]. WISP1 is expressed in the epithelium, heart, kidney, lung, pancreas, placenta, ovaries, small intestine, and spleen with limited brain expression [4].

WISP1 is considered a target of Wnt1 [5]. Given that Wnt1 is a cysteine-rich glycosylated protein that controls neuronal development, cell growth, and neuronal cell survival [6–13], it is conceivable to consider that cytoprotection by Wnt1 may be mediated by WISP1. In addition, Wnt1 has recently been shown to require pathways of phosphoinositide 3-kinase (PI 3-K) and Akt1 to promote cytoprotection and prevent apoptotic cell death [6, 8, 14–16]. In this apoptotic cascade, Akt1 has been shown to affect mitochondrial membrane permeability, cytochrome c release, and caspase activation [14, 17–21]. WISP1 in cells exclusive of the nervous system uses PI 3-K and Akt signaling to promote cell survival and cell proliferation [22–25].

In light of the potential role for WISP1 to avert neurodegeneration, we investigated the ability of WISP1 to prevent primary neuronal injury and apoptosis during oxidative stress using oxygen-glucose deprivation (OGD) in primary hippocampal neurons. We demonstrate that WISP1 is expressed in primary neurons during OGD exposure and that Wnt1 increases and maintains the expression of WISP1 during oxidative stress. Similar to Wnt1, WISP1 blocks primary neuronal injury and apoptotic degeneration through pathways that require PI 3-K and Akt1 activation. Downstream from PI 3-K and Akt1, WISP1 phosphorylates Bad and GSK-3β through the activation of PI 3-K and Akt1 and reduces the expression of the Bim/Bax complex and increases the expression of Bcl-x_L/Bax complex in neurons, events that can foster neuronal survival during oxidative stress. WISP1 also prevents the loss of mitochondrial membrane permeability, cytochrome c release, and caspase 3 activity during OGD which are dependent upon the PI 3-K and Akt1 pathways. Our work offers new insights into the potential role of WISP1 during neurodegeneration and the cellular pathways controlled by WISP1 to foster neuronal viability.

MATERIALS AND METHODS

Hippocampal Neuronal Cultures

Per our prior protocols [8, 18, 26, 27], hippocampi were obtained from E-19 Sprague-Dawley rat pups and incubated in Hanks' balanced salt solution (HBBS) supplemented with 1 mM sodium pyruvate and 10 mM HEPES buffer solution (Invitrogen, Carlsbad, CA). The neurons were isolated by trituration for 10 times, centrifuged for 2 min at 200 g and then dissociated in growth medium (Leibovitz's L-15 medium, Invitrogen, Carlsbad, CA) containing 6% sterile rat serum (ICN, Aurora, OH), 150 mM $NaHCO_3$, 2.25 mg/ml of transferrin, 2.5 μg/ml of insulin, 10 nM progesterone, 90 μM putrescine, 15 nM selenium, 35 mM glucose, 1 mM L-glutamine, penicillin and streptomycin (50 μg/ml), and vitamins. Cells were then plated at a density of ~1.5×10^3cells/mm^2 in 35 mm polylysine/laminin-coated plates (Falcon Labware, Lincoln Park, NJ). Neurons were maintained in growth medium at 37 °C in a humidified atmosphere of 5% CO_2 and 95% room air for 10–14 days.

Experimental Treatments

Per our prior protocols, oxygen-glucose deprivation (OGD) in microglia was performed by replacing the media with glucose-free HBSS containing 116 mmol/l NaCl, 5.4 mmol/l KCl, 0.8 mmol/l $MgSO_4$, 1 mmol/l NaH_2PO_4, 0.9 mmol/l $CaCl_2$, and 10 mg/l phenol red (pH 7.4) and cultures were maintained in an anoxic environment (95% N_2 and 5% CO_2) at 37 °C per our prior experimental paradigms [28–30]. For treatments applied prior to OGD, human recombinant Wnt1 protein (R&D Systems, Minneapolis, MN) and human recombinant WISP1 protein (R&D Systems, Minneapolis, MN) were continuous. PI-3K and Akt pathway inhibition was performed by administering wortmannin (0.5 μM, Calbiochem, La Jolla, CA) or LY294002 (Sigma, St Louis, MO) directly to the cultures 1 hour prior to OGD.

Assessment of Cell Survival

Neuronal cell injury was determined by bright field microscopy using a 0.4% trypan blue dye exclusion method 24 hours following treatment with OGD per our previous protocols [20, 31]. The mean survival was determined by counting eight randomly selected non-overlapping fields with each containing approximately 10–20 cells (viable + non-viable). Each experiment was replicated 4–6 times with different cultures

Assessment of DNA Fragmentation

Genomic DNA fragmentation was determined by the terminal deoxynucleotidyl transferase nick end labeling (TUNEL) assay [19, 32]. Briefly, neuronal cells were fixed in 4% paraformaldehyde/0.2% picric acid/0.05% glutaraldehyde and the 3′-hydroxy ends of cut DNA were labeled with biotinylated dUTP using the enzyme terminal deoxytransferase (Promega, Madison, WI) followed by streptavidin-peroxidase and visualized with 3,3′-diaminobenzidine (Vector Laboratories, Burlingame, CA).

Assessment of Mitochondrial Membrane Potential

The fluorescent probe JC-1 (Molecular Probes, Eugene, OR), a cationic membrane potential indicator, was used to assess the mitochondrial membrane potential [18, 33]. Neuronal cells in 35 mm^2 dishes were incubated with 2 μg/ml JC-1 in growth medium at 37 °C for 30 min. The cultures were washed three times using fresh growth medium. Mitochondria were then analyzed immediately under a Leitz DMIRB microscope (Leica, McHenry, IL, USA) with a dual emission fluorescence filter with 515–545 nm for green fluorescence and emission at 585–615 nm for red fluorescence [31].

Expression of Phosphorylated Akt1, WISP1, Glycogen Synthase Kinase-3β (GSK-3β), Bad Bax, Bim, Bcl-xL, and Cytochrome c, and Caspase 3

Cell protein extracts were subjected to SDS-PAGE (7.5%, Akt1; 12.5%, WISP1, GSK-3β, Bad Bax, Bim, Bcl-xL, cytochrome c, and caspase 3) separation. After blocking for 1 hour at room temperature with 5% skim milk, the membranes were incubated overnight at 4 °C with a rabbit polyclonal antibody against WISP1 (1:200, Santa Cruz Biotechnologies, Santa Cruz, CA), a rabbit polyclonal antibody against phospho-Akt1 (p-Akt1, Ser^{473}, 1:1000, Cell Signaling, Beverly, MA), a rabbit monoclonal antibody against phospho-Bad (p-Bad, Ser^{136}, 1:1000, Cell Signaling, Beverly, MA), a rabbit polyclonal antibody against phospho-GSK-3β (p-GSK-3β, Ser^{9}, 1:1000), cytochrome c (1:1000), cleaved (active) caspase 3 (17 kDa) (1:1000) (Cell signaling, Beverly, MA), a rabbit polyclonal antibody against Bim (1:100, Calbiochem, San Diego, CA), a rabbit polyclonal antibody against Bcl-x_L (1:1000, Cell Signaling, Beverly, MA). After incubation of the membranes with horseradish peroxidase conjugated secondary antibody (goat anti-mouse IgG, 1:5000) (Pierce, Rockford, IL), the antibody-reactive bands were revealed by enhanced chemiluminescence detection on Hyperfilm (Amersham Pharmacia Biotech, Piscataway, NJ).

Preparation of Mitochondria for the Analysis of Cytochrome c Release

After washing once with ice-cold PBS, cells were harvested at 10,000g for 15 min at 4°C and the resulting pellet was re-suspended in buffer A (20 mM HEPES, pH 7.5, 10 mM KCl, 1.5 mM MgCl2, 1 mM EDTA, 1 mM EGTA, 1 mM dithiothreitol, 0.1 phenylmethylsulfonylfluoride) containing 250 mM sucrose and used as the mitochondrial fraction. The supernatant was subjected to ultracentrifugation at 50,000 g for 1 hour at 4 °C with the resultant supernatant used as the cytosolic fraction [34, 35].

Immunoprecipitation for Bim and Bcl-x_L Binding Activity to Bax

Cell lysates of total protein (200 μg) were incubated with antibody against protein Bax (1:1000, Cell Signaling, Beverly, MA) overnight at 4°C. The complexes were collected with protein A/G-agarose beads, centrifuged and then prepared for Bim and Bcl-x_L Western analysis.

Statistical Analysis

For each experiment, the mean and standard error were determined. Statistical differences between groups were assessed by means of analysis of variance (ANOVA) from 4–6 replicate experiments with the post-hoc Dunnett's test. Statistical significance was considered at $P<0.05$.

RESULTS

Wnt1 Blocks Neuronal Injury During OGD

Neuronal cells were initially exposed to OGD for 2, 3 or 4 hours and cell injury was determined by the trypan blue (TB) exclusion method and TUNEL analysis 24 hours later. As shown in Fig. (1A), representative pictures demonstrate that OGD at 2, 3 or 4 hors results in the loss of membrane integrity with staining in a significant number of neuronal cells with trypan blue and DNA fragmentation. The quantitative results in Fig. 1B demonstrated that neuronal labeling was significantly increased to 22 ± 1% (2 hours, TB), 21 ± 2% (2 hours, TUNEL), 44 ± 2% (3 hours, TB), 45 ± 3% (3 hours, TUNEL), 73 ± 2% (4 hours, TB), and 73 ± 1% (4 hours, TUNEL) 24 hours following OGD exposure when compared to untreated control cultures (3 ± 1%, TB) and (3 ± 1%, TUNEL). Since an OGD exposure period of 3 hours resulted in survival rate of approximately 45% neuronal cell loss (55% die), this duration of exposure to OGD was used for the remainder of the experiments.

To determine whether Wnt1, an upstream mediator of WISP1, could protect neurons against OGD, Wnt1 (20, 50, 100 and 150 ng/ml) was applied to neuronal cultures 1 hour prior to a 3 hour period of OGD and cell injury was determined 24 hours after OGD by the trypan blue (TB) exclusion method and apoptotic DNA fragmentation (TUNEL). As shown in Fig. (1C), Wnt1 (100 or 150 ng/ml) significantly reduced trypan blue uptake and DNA fragmentation in neuronal cells. The quantitative results in Fig. (1D) demonstrated that the percent cell labeling of typan blue and TUNEL was significantly decreased to 40 ± 2% and 40 ± 3% by 100 ng/ml Wnt1 administration respectively. Wnt1 (150 ng/ml) did not further reduce percent trypan blue staining or DNA fragmentation when compared with the concentration of Wnt1 100 ng/ml. As a result, a Wnt1 concentration of 100 ng/ml was used in subsequent experimental protocols. Wnt1 at the concentrations less than 100 ng/ml did not significantly protect against cell injury.

Wnt1 Increases and Maintains WISP1 Expression During OGD

To investigate the ability of Wnt1 to alter the expression of WISP1 in neurons following OGD, hippocampal neurons protein extracts (50 μg/lane) were immunoblotted with anti-

WISP1 antibody at 1, 3, and 24 hours following a 3 hour period of OGD. As shown in Fig. (2A), WISP1 expression was mildly increased at 1, 3 and 24 hours following OGD demonstrating the presence of WISP1 in primary neurons. Application of Wnt1 (100 ng/ml) 1 hour prior to OGD significantly increased the expression of WISP1 in neurons over a 24 hour period to a greater degree than OGD alone (Fig. 2A).

WISP1 Prevents Neuronal Cell Injury and Apoptosis During OGD Exposure

Recombinant human WISP1 protein (1–20 ng/ml) was applied to neuronal cultures 1 hour prior to a 3 hour period of OGD and cell injury was determined 24 hours following OGD by using trypan blue exclusion method and TUNEL assay. In Fig. (2B), representative pictures demonstrate that untreated neuronal cells were without evidence of trypan blue uptake and nuclear DNA damage, but exposure to OGD resulted in significant trypan blue staining and nuclear DNA damage 24 hours following OGD. In contrast, cells exposed to WISP1 (10–20 ng/ml) had significantly reduced trypan blue staining and DNA degradation. Quantitative results illustrate that percent trypan blue staining and DNA fragmentation were significantly increased in neurons 24 hours following OGD. In contrast, cells receiving either WISP1 (10 ng/ml) or WISP1 (20 ng/ml) had significantly reduced percent trypan blue staining and DNA fragmentation to an almost similar degree of protection (Fig. 2B).

WISP1 Requires PI 3-K and Akt1 During OGD to Foster Neuronal Protection

To investigate the effects of WISP1 on the PI 3-K and Akt1 pathways, western blot assay was performed for phosphorylated Akt1 (p-Akt1) (activated form of Akt1) at 1, 3 and 24 hours after administration of 5 ng/ml, 10 ng/ml, or 20 ng/ml WISP1 to neurons. WISP1 significantly enhanced p-Akt1 expression in a concentration dependent manner. As shown in Fig. (3A), WISP1 at the concentration of 5 ng/ml significantly increased the expression of p-Akt1 after 3 hours incubation. At higher concentrations, WISP1 (10–20 ng/ml) increased phosphorylation of Akt1 at 1, 3, and 24 hours (20 ng/ml concentration only). The maximal increased expression of phosphorylated Akt1 was observed at the 3 hour time point for WISP1 (10 ng/ml). Expression of p-Akt1 returned to the level of control cells 24 hours following administration of WISP1. In Fig. (3B), expression of p-Akt1 was increased 1 and 3 hours following a 3 hour period of OGD. In contrast, WISP1 (10 ng/ml) increased and maintained the expression of phosphorylated Akt1 at 1 hour and 3 hours following OGD exposure. However, the ability of WISP1 to significantly increase phosphorylated Akt1 expression was lost during application of the PI 3-K inhibitors wortmannin (0.5 μM) or LY294002 (10 μM) (Fig. 3C). The inhibitor wortmannin (0.5 μM) forms a covalent link with the lysine residue of PI 3-K [36] and the inhibitor LY294002 (10 μM) reversibly competes for ATP binding [37].

We next assessed whether WISP1 required the PI 3-K pathway to prevent neuronal cell injury and apoptosis. Neuronal cell injury was determined by the trypan blue dye exclusion method and TUNEL analysis 24 hours following a 3 hour exposure period of OGD. Representative images and quantitative results demonstrate that WISP (10 ng/ml) applied 1 hour prior to OGD significantly reduced trypan blue staining and DNA fragmentation in neurons (Fig. 3D). Yet, administration of either the PI 3-K inhibitor wortmannin (0.5 μM) or LY294002 (10 μM) with WISP1 (10 ng/ml) blocked the ability of WISP1 to prevent neuronal cell injury or apoptosis during OGD exposure, suggesting the PI 3-K and Akt1 pathways were necessary for WISP1 neuronal protection. Furthermore, application of wortmannin (0.5 μM) or LY294002 (10 μM) increased cell injury during OGD, illustrating that an endogenous level of PI 3-K provides protection to neuronal cells during toxic environmental exposure.

WISP1 Utilizes PI 3-K to Control Phosphorylation of Bad and GSK-3β During OGD

We next examined the effects of WISP1 on the phospho-rylation of Bad and GSK-3β, since the phosphorylation sites of Bad (Ser^{136}) and GSK-3β (Ser^{9}) are downstream targets of Akt1. WISP1 (10 ng/ml) applied 1 hour prior to a 3 hour period of OGD significantly increased the expression of p-Bad and p-GSK-3β 3 hours following OGD (Fig. 4A and 4B). However, the ability of WISP1 (10 ng/ml) to phos-phorylate p-Bad or p-GSK-3β during OGD exposure was lost with the application of the PI 3-K inhibitors wortmannin (0.5 μM) or LY294002 (10 μM), suggesting that WISP1 phosphorylates Bad and GSK-3β through PI 3-K and Akt1 activation. In addition, application of wortmannin (0.5 μM) or LY294002 (10 μM) further decreased phosphorylation of p-Bad or p-GSK-3β during OGD, illustrating that an endogenous level of PI 3-K and Akt1 provides a level of phosphorylation of these proteins during OGD exposure.

WISP1 Dissociates Bim from Bax and Increases the Binding of Bcl-x_L to Bax

We subsequently investigated the ability of WISP1 to alter Bax and Bim binding as well as the association between Bcl-x_L and Bax. WISP1 (10 ng/ml) was administered 1 hour prior to a 3 hour period of OGD and primary neuronal cell extracts at 3 hours following OGD were immunoprecipited using an antibody to Bax. As shown in Fig. (5A) and Fig. (5B), representative western blots for Bim and Bcl-x_L immunoprecipitation demonstrates that OGD alone resulted in a significant increase in the expression of the Bim/Bax complex and a significant decrease in the expression of Bcl-x_L/Bax complex when compared with untreated control cultures. In contrast, WISP1 significantly reduced the expression of the Bim/Bax complex and increased the expression of Bcl-x_L/Bax complex in neuronal precipitates.

WISP1 Prevents Mitochondrial Membrane Depolarization, Cytochrome c Release, and the Activation of Caspase 3 through PI 3-K and Akt1 Pathways During OGD

We next examined the ability of WISP1 to influence mitochondrial membrane permeability, cytochrome c release, and the activation of caspase 3 as well as the dependence of WISP1 on PI 3-K and Akt1 to control these pathways. In Fig. (6A), OGD exposure yielded a significant decrease in the neuronal mitochondrial red/green fluorescence intensity ratio at 3 hours after a 3 hour period of OGD when compared to untreated control neurons, suggesting that OGD exposure results in mitochondrial membrane depolarization. WISP1 (10 ng/ml) administration 1 hour prior to OGD exposure significantly increased the red/green fluorescence intensity of the mitochondria, illustrating that WISP1 can significantly improve mitochondrial permeability transition pore membrane potential. Application of the specific PI 3-K inhibitors wortmannin (0.5 μM) or LY294002 (10 μM) 1 hour prior to a 3 hour period of OGD prevented WISP1 from maintaining mitochondrial membrane potential, illustrating that WISP1 is dependent upon the PI 3K/Akt1 pathways to control mitochondrial membrane permeability during OGD exposure. In addition, wortmannin (0.5 μM) or LY294002 (10 μM) further enhanced mitochondrial membrane permeability during OGD, suggesting that a baseline cellular level of PI 3-K/Akt1 assists with maintenance of mitochondrial membrane permeability during OGD exposure.

Subsequent cytochrome c release from mitochondria was evaluated by western blot for cytochrome c expression in both mitochondrial and cytosol extractions. As shown in Fig. (6B), OGD produced a significant increase in the release of cytochrome c from the mitochondria revealed by increased expression of cytochrome c in the cytosol. Yet, WISP1 (10 ng/ml) administration prevented cytochrome c release and decreased the expression of cytochrome c in the cytosol. Furthermore, administration of wortmannin (0.5 μM) or LY294002 (10 μM) in combination with WISP1 (10ng/ml) prevented WISP1 from

controlling cytochrome c release during OGD exposure, illustrating that PI 3-K and Akt1 pathways are necessary for WISP1 to prevent cytochrome c release (Fig. 6B).

We next examined the ability of WISP1 to modulate caspase 3 activity. In Fig. (6C), the expression of cleaved (active) caspase 3 on western analysis were significantly increased at 3 hours after a 3 hour period of OGD exposure. WISP1 (10 ng/ml) applied 1 hour prior to OGD significantly blocked caspase 3 activity during OGD. In contrast, WISP1 could not alter caspase 3 activity during OGD when administration of wortmannin (0.5 μM) or LY294002 (10 μM) was present (Fig. 6C).

DISCUSSION

Wnt1 is a cysteine-rich glycosylated protein [3, 7, 38] that controls neuronal proliferation [39] as well as neural stem cell development [40]. In mature neurons, Wnt1 has recently been shown to protect against ischemic cortical injury [8], foster neuronal survival during amyloid exposure [6], potentially suppress the onset or progression of Alzheimer's disease [13], and promote neuronal cell and astrocyte crosstalk as a mechanism of neuroprotection [10, 41]. Furthermore, cytoprotecion by Wnt1 extends to vascular cells [14, 16, 42–44] that also can support neuronal survival.

Although Wnt1 may employ a variety of pathways to offer neuronal protection [6, 8, 14, 16, 41, 43, 45, 46], WISP1 may represent an important target of Wnt1 that is responsible for cellular protection [5], especially in neurons. We demonstrate that Wnt1 provides significant protection against neuronal cell injury and apoptosis during oxidant stress with OGD exposure. Maximum protection with Wnt1 was achieved at a concentration of 100 ng/ml similar to other injury protocols demonstrating Wnt1 cytoprotection at a concentration of 100 ng/ml in microglia [16, 43], vascular cells [14, 42], and neurons [6, 8, 10].

Interestingly, WISP1 is expressed in primary brain neurons. Both Wnt1 with OGD and OGD alone resulted in the increased expression of WISP1. However, Wnt1 significantly increased WISP1 expression to a greater degree than OGD alone and maintained the expression of WISP1 in primary neurons over a 24 hour period during oxidative stress. Previously, Wnt1 has been associated with the increased expression of WISP1 in human vascular smooth muscle cells during aging [47]. In conjunction with these prior studies, our current work suggests that WISP1 may represent a vital component for cell protection in the Wnt1 signaling pathway. WISP1 in tumors may mediate the anti-apoptotic effects of Wnt1 [5] and WISP1 can prevent doxorubicin-induced cardiomyocyte death [25]. WISP1 is expressed during epithelial lung stretch injury [48], during fracture repair to promote mesenchymal cell proliferation [49], and during crush injury in human saphenous veins [50], suggesting a number of scenarios for WISP1 to enhance cell survival. We therefore investigated the ability of WISP1 to block neurodegeneration during oxidative stress. We show that WISP1 in a concentration dependent manner significantly reduces neuronal cell injury and prevents apoptotic nuclear DNA degradation during oxidative stress. Maximum survival occurred with WISP1 concentrations of 10 ng/ml and 20 ng/ml similar to studies in the cardiovascular system [25, 51]. Considering that oxidative stress can promote processes of aging as well as lead to debilitating injury in multiple systems of the body that include the nervous system, vascular system, and immune system [52–61], WISP1 cytoprotection may provide an interesting therapeutic avenue for multiple disorders that extend beyond the nervous system.

WISP1 promotes cytoprotection in primary neurons through PI 3-K and Akt1 pathways. PI 3-K and especially Akt1 are central to the regulation of cell growth and survival throughout the body [14, 30, 34, 43, 62–71]. WISP1 in non-neuronal systems has been shown to rely upon the PI 3-K and Akt signaling [22–25]. Furthermore, Wnt1, which we have shown in

the current study can control the expression of WISP1 in neuronal cells, also has been shown to utilize Akt1 [6, 8, 14–16]. In primary neuronal cells, WISP1 promotes and maintains the phosphorylation of Akt1 during the initial onset of OGD exposure which may be critical for the downstream modulation of mitochondrial permeability, cytochrome c release, and caspase activation. The PI 3-K and Akt1 pathways appear to be vital for WISP1 neuronal protection, since administration of either the PI 3-K inhibitor wortmannin or LY294002 with WISP1 blocked the ability of WISP1 to prevent neuronal cell injury or apoptosis during OGD exposure. In addition, similar to prior studies in neurons, vascular cells and inflammatory cells [32, 43, 72], inhibition of the PI 3-K and Akt1 pathways alone during OGD exposure resulted in an increase in neuronal cell injury and in neuronal apoptosis, demonstrating that primary neurons rely upon an endogenous level of activity of PI 3-K and Akt1 to assist with cell survival during toxic environments.

Dependence upon PI 3-K and Akt1 for WISP1 extend to the ability of WISP1 to modulate other downstream pathways such as those of Bad, GSK-3β, Bim, and Bcl-x_L. Bad is a pro-apoptotic Bcl-2 family member that becomes active through phosphorylation on its serine residues [64, 73]. Phosphorylation of Bad by Akt leads to the binding of Bad with the cytosolic protein 14-3-3 to release Bcl-x_L to block apoptosis by allowing association of Bcl-x_L to the pro-apoptotic protein Bax [30, 68, 74–76]. Bcl-2 and Bcl-x_L block Bax translocation to the mitochondria, maintain mitochondrial membrane potential, and prevent the release of cytochrome c from the mitochondria [77]. Apoptosis also can be triggered through the transcription of the pro-apoptotic gene Bim. Bim, a BH3-only Bcl-2 family member, functions upstream of Bax-mediated cytochrome c release from the mitochondria [56, 78]. Although Wnt1 has previously be demonstrated to phosphorylate Bad [16], we now show that WISP1 phosphorylates Bad and GSK-3β through the activation of PI 3-K and Akt1 as well as illustrate that an endogenous level of PI 3-K and Akt1 provides a level of phosphorylation of these proteins during OGD exposure alone. Furthermore, WISP1 significantly reduced the expression of the Bim/Bax complex and increased the expression of Bcl-x_L/Bax complex in neurons, suggesting that WISP1 prevents neuronal apoptosis by promoting expression of a Bcl-x_L/Bax complex and limiting the expression of a Bim/Bax complex [79].

However, if Bax remains unchecked and does not form a complex with Bcl-x_L, Bax can then lead to increased mitochondrial membrane permeability, the release of cytochrome c, and subsequent caspase 3 activation [55, 80]. In addition, given the dependence of WISP1 on the PI 3-K and Akt1 pathways, it is known that the cytoprotective pathways promoted by PI 3-K and Akt1 have been tied to the modulation of mitochondrial permeability and cytochrome c release [14, 30, 66, 69, 71]. We therefore examined the ability of WISP1 to modulate mitochondrial membrane permeability and related apoptotic pathways. WISP1 maintained mitochondrial permeability transition pore membrane potential and prevented cytochrome c release during OGD which were dependent upon the PI 3K and Akt1 pathways.

Given that WISP1 can maintain mitochondrial membrane permeability and prevent cytochrome c release, processes that ultimately if remain unabated lead to caspase 3 activation [16, 30, 32, 33, 81–86], we also examined the ability of WISP1 to modulate caspase 3 activity in primary neurons. WISP1 significantly prevented caspase 3 activity during OGD. Prevention of caspase 3 activation by WISP1 also was dependent upon the activity of the PI 3-K and Akt1 pathways.

Our present studies suggest that WISP1 may offer novel therapeutic strategies for neurodegenerative disorders. Wnt1, previously demonstrated to be cytoprotective in several cell systems, can control the expression of WISP1 during oxidative stress. WISP1 promotes primary neuronal survival and blocks apoptotic demise through PI 3-K and Akt1 pathways

that ultimately control the downstream pathways of Bad, GSK-3β, Bim, Bcl-x_L, mitochondrial membrane permeability, cytochrome c release, and caspase 3 activation. Yet, further investigative studies for WISP1 are clearly indicated. Similar to other growth promoting agents [87–90], WISP1 has been associated with tumorigenesis in esophageal carcinoma [91], in chondrosarcoma [92], and in colorectal cancer [93]. Future work that can further elucidate pathways governed by WISP1 that oversee cellular survival and growth will prove to be invaluable in determining effective and safe applications for WISP1 not only in neurodegenerative disorders, but also in diseases involving other systems of the body.

Acknowledgments

This research was supported by the following grants to Kenneth Maiese: American Diabetes Association, American Heart Association (National), Bugher Foundation Award, LEARN Foundation Award, NIH NIEHS, NIH NIA, NIH NINDS, and NIH ARRA.

References

1. Berschneider B, Konigshoff M. WNT1 inducible signaling pathway protein 1 (WISP1): a novel mediator linking development and disease. Int J Biochem Cell Biol. 2010; 43(3):306–9. [PubMed: 21109017]
2. Jun JI, Lau LF. Taking aim at the extracellular matrix: CCN proteins as emerging therapeutic targets. Nat Rev Drug Discov. 2011; 10(12):945–63. [PubMed: 22129992]
3. Maiese K, Li F, Chong ZZ, Shang YC. The Wnt signaling pathway: Aging gracefully as a protectionist? Pharmacol Ther. 2008; 118(1):58–81. [PubMed: 18313758]
4. Pennica D, Swanson TA, Welsh JW, et al. WISP genes are members of the connective tissue growth factor family that are up-regulated in wnt-1-transformed cells and aberrantly expressed in human colon tumors. Proc Natl Acad Sci USA. 1998; 95(25):14717–22. [PubMed: 9843955]
5. You Z, Saims D, Chen S, Zhang Z, Guttridge DC, Guan KL, et al. Wnt signaling promotes oncogenic transformation by inhibiting c-Myc-induced apoptosis. J Cell Biol. 2002; 157(3):429–40. [PubMed: 11980918]
6. Chong ZZ, Li F, Maiese K. Cellular demise and inflammatory microglial activation during beta-amyloid toxicity are governed by Wnt1 and canonical signaling pathways. Cell Signal. 2007; 19(6): 1150–62. [PubMed: 17289346]
7. Chong ZZ, Maiese K. Targeting WNT, protein kinase B, and mitochondrial membrane integrity to foster cellular survival in the nervous system. Histol Histopathol. 2004; 19(2):495–504. [PubMed: 15024710]
8. Chong ZZ, Shang YC, Hou J, Maiese K. Wnt1 neuroprotection translates into improved neurological function during oxidant stress and cerebral ischemia through AKT1 and mitochondrial apoptotic pathways. Oxid Med Cell Longev. 2010; 3(2):153–65. [PubMed: 20716939]
9. Fernandez-Martos CM, Gonzalez-Fernandez C, Gonzalez P, Maqueda A, Arenas E, Rodriguez FJ. Differential expression of wnts after spinal cord contusion injury in adult rats. PLoS ONE. 2011; 6(11):e27000. [PubMed: 22073235]
10. L'Episcopo F, Serapide MF, Tirolo C, et al. A Wnt1 regulated Frizzled-1/beta-Catenin signaling pathway as a candidate regulatory circuit controlling mesencephalic dopaminergic neuron-astrocyte crosstalk: Therapeutical relevance for neuron survival and neuroprotection. Molecular neurodegeneration. 2011; 6:49. [PubMed: 21752258]
11. Maiese K. Triple play: Promoting neurovascular longevity with nicotinamide, WNT, and erythropoietin in diabetes mellitus. Biomed Pharmacother. 2008; 62(4):218–32. [PubMed: 18342481]
12. Okerlund ND, Cheyette BN. Synaptic Wnt signaling-a contributor to major psychiatric disorders? J Neurodev Disord. 2011; 3(2):162–74. [PubMed: 21533542]

13. Wexler EM, Rosen E, Lu D, et al. Genome-wide analysis of a wnt1-regulated transcriptional network implicates neurodegenerative pathways. Science signaling. 2011; 4(193):ra65. [PubMed: 21971039]

14. Chong ZZ, Hou J, Shang YC, Wang S, Maiese K. EPO Relies upon Novel Signaling of Wnt1 that Requires Akt1, FoxO3a, GSK-3beta, and beta-Catenin to Foster Vascular Integrity During Experimental Diabetes. Curr Neurovasc Res. 2011; 8(2):103–20. [PubMed: 21443457]

15. Longo KA, Kennell JA, Ochocinska MJ, Ross SE, Wright WS, MacDougald OA. Wnt signaling protects 3T3-L1 preadipocytes from apoptosis through induction of insulin-like growth factors. J Biol Chem. 2002; 277(41):38239–44. [PubMed: 12154096]

16. Shang YC, Chong ZZ, Hou J, Maiese K. Wnt1, FoxO3a, and NF-kappaB oversee microglial integrity and activation during oxidant stress. Cell Signal. 2010; 22(9):1317–29. [PubMed: 20462515]

17. Campos-Esparza MR, Sanchez-Gomez MV, Matute C. Molecular mechanisms of neuroprotection by two natural antioxidant polyphenols. Cell Calcium. 2009; 45(4):358–68. [PubMed: 19201465]

18. Chong ZZ, Lin SH, Li F, Maiese K. The sirtuin inhibitor nicotinamide enhances neuronal cell survival during acute anoxic injury through Akt, Bad, PARP, and mitochondrial associated “anti-apoptotic” pathways. Curr Neurovasc Res. 2005; 2(4):271–85. [PubMed: 16181120]

19. Hou J, Chong ZZ, Shang YC, Maiese K. Early apoptotic vascular signaling is determined by Sirt1 through nuclear shuttling, forkhead trafficking, bad, and mitochondrial caspase activation. Curr Neurovasc Res. 2010; 7(2):95–112. [PubMed: 20370652]

20. Kang JQ, Chong ZZ, Maiese K. Akt1 protects against inflammatory microglial activation through maintenance of membrane asymmetry and modulation of cysteine protease activity. J Neurosci Res. 2003; 74(1):37–51. [PubMed: 13130504]

21. Kennedy SG, Kandel ES, Cross TK, Hay N. Akt/Protein kinase B inhibits cell death by preventing the release of cytochrome c from mitochondria. Mol Cell Biol. 1999; 19(8):5800–10. [PubMed: 10409766]

22. Colston JT, de la Rosa SD, Koehler M, et al. Wnt-induced secreted protein-1 is a prohypertrophic and profibrotic growth factor. Am J Physiol Heart Circ Physiol. 2007; 293(3):H1839–46. [PubMed: 17616748]

23. Reddy VS, Valente AJ, Delafontaine P, Chandrasekar B. Interleukin-18/WNT1-inducible signaling pathway protein-1 signaling mediates human saphenous vein smooth muscle cell proliferation. J Cell Physiol. 2011; 226(12):3303–15. [PubMed: 21321938]

24. Su F, Overholtzer M, Besser D, Levine AJ. WISP-1 attenuates p53-mediated apoptosis in response to DNA damage through activation of the Akt kinase. Genes Dev. 2002; 16(1):46–57. [PubMed: 11782444]

25. Venkatesan B, Prabhu SD, Venkatachalam K, et al. WNT1-inducible signaling pathway protein-1 activates diverse cell survival pathways and blocks doxorubicin-induced cardiomyocyte death. Cell Signal. 2010; 22(5):809–20. [PubMed: 20074638]

26. Chong ZZ, Kang JQ, Maiese K. Erythropoietin fosters both intrinsic and extrinsic neuronal protection through modulation of microglia, Akt1, Bad, and caspase-mediated pathways. Br J Pharmacol. 2003; 138(6):1107–18. [PubMed: 12684267]

27. Chong ZZ, Li F, Maiese K. Erythropoietin requires NF-kappaB and its nuclear translocation to prevent early and late apoptotic neuronal injury during beta-amyloid toxicity. Curr Neurovasc Res. 2005; 2(5):387–99. [PubMed: 16375720]

28. Chong ZZ, Li F, Maiese K. The pro-survival pathways of mTOR and protein kinase B target glycogen synthase kinase-3beta and nuclear factor-kappaB to foster endogenous microglial cell protection. Int J Mol Med. 2007; 19(2):263–72. [PubMed: 17203200]

29. Chong ZZ, Maiese K. Erythropoietin involves the phosphatidylinositol 3-kinase pathway, 14-3-3 protein and FOXO3a nuclear trafficking to preserve endothelial cell integrity. Br J Pharmacol. 2007; 150(7):839–50. [PubMed: 17339844]

30. Hou J, Wang S, Shang YC, Chong ZZ, Maiese K. Erythropoietin Employs Cell Longevity Pathways of SIRT1 to Foster Endothelial Vascular Integrity During Oxidant Stress. Curr Neurovasc Res. 2011; 8(3):220–35. [PubMed: 21722091]

31. Kang JQ, Chong ZZ, Maiese K. Critical role for Akt1 in the modulation of apoptotic phosphatidylserine exposure and microglial activation. Mol Pharmacol. 2003; 64(3):557–69. [PubMed: 12920191]
32. Chong ZZ, Kang JQ, Maiese K. AKT1 drives endothelial cell membrane asymmetry and microglial activation through Bcl-xL and caspase 1, 3, and 9. Exp Cell Res. 2004; 296(2):196–207. [PubMed: 15149850]
33. Chong ZZ, Lin SH, Maiese K. Nicotinamide Modulates Mitochondrial Membrane Potential and Cysteine Protease Activity during Cerebral Vascular Endothelial Cell Injury. J Vasc Res. 2002; 39(2):131–47. [PubMed: 12011585]
34. Chong ZZ, Kang JQ, Maiese K. Erythropoietin is a novel vascular protectant through activation of Akt1 and mitochondrial modulation of cysteine proteases. Circulation. 2002; 106(23):2973–9. [PubMed: 12460881]
35. Hou J, Chong ZZ, Shang YC, Maiese K. FoxO3a governs early and late apoptotic endothelial programs during elevated glucose through mitochondrial and caspase signaling. Mol Cell Endocrinol. 2010; 321(2):194–206. [PubMed: 20211690]
36. Wymann MP, Bulgarelli-Leva G, Zvelebil MJ, et al. Wortmannin inactivates phosphoinositide 3-kinase by covalent modification of Lys-802, a residue involved in the phosphate transfer reaction. Mol Cell Biol. 1996; 16(4):1722–33. [PubMed: 8657148]
37. Vlahos CJ, Matter WF, Hui KY, Brown RF. A specific inhibitor of phosphatidylinositol 3-kinase, 2-(4-morpholinyl)-8-phenyl-4H-1-benzopyran-4-one (LY294002). J Biol Chem. 1994; 269(7): 5241–8. [PubMed: 8106507]
38. Li F, Chong ZZ, Maiese K. Vital elements of the wnt-frizzled signaling pathway in the nervous system. Curr Neurovasc Res. 2005; 2(4):331–40. [PubMed: 16181124]
39. Panhuysen M, Vogt Weisenhorn DM, Blanquet V, et al. Effects of Wnt1 signaling on proliferation in the developing mid-/hindbrain region. Mol Cell Neurosci. 2004; 26(1):101–11. [PubMed: 15121182]
40. Sieber-Blum M. Ontogeny and plasticity of adult hippocampal neural stem cells. Dev Neurosci. 2003; 25(2–4):273–8. [PubMed: 12966223]
41. L'Episcopo F, Tirolo C, Testa N, et al. Reactive astrocytes and Wnt/beta-catenin signaling link nigrostriatal injury to repair in 1-methyl-4-phenyl-1,2,3,6-tetrahydropyridine model of Parkinson's disease. Neurobiol Dis. 2011; 41(2):508–27. [PubMed: 21056667]
42. Chong ZZ, Shang YC, Maiese K. Vascular injury during elevated glucose can be mitigated by erythropoietin and Wnt signaling. Curr Neurovasc Res. 2007; 4(3):194–204. [PubMed: 17691973]
43. Shang YC, Chong ZZ, Wang S, Maiese K. Erythropoietin and Wnt1 Govern Pathways of mTOR, Apaf-1, and XIAP in Inflammatory Microglia. Curr Neurovasc Res. 2011; 8(4):270–85. [PubMed: 22023617]
44. Woll PS, Morris JK, Painschab MS, et al. Wnt signaling promotes hematoendothelial cell development from human embryonic stem cells. Blood. 2008; 111(1):122–31. [PubMed: 17875805]
45. Bournat JC, Brown AM, Soler AP. Wnt-1 dependent activation of the survival factor NF-kappaB in PC12 cells. J Neurosci Res. 2000; 61(1):21–32. [PubMed: 10861796]
46. Castilho RM, Squarize CH, Chodosh LA, Williams BO, Gutkind JS. mTOR mediates Wnt-induced epidermal stem cell exhaustion and aging. Cell Stem Cell. 2009; 5(3):279–89. [PubMed: 19733540]
47. Marchand A, Atassi F, Gaaya A, et al. The Wnt/beta-catenin pathway is activated during advanced arterial aging in humans. Aging Cell. 2011; 10(2):220–32. [PubMed: 21108734]
48. Heise RL, Stober V, Cheluvaraju C, Hollingsworth JW, Garantziotis S. Mechanical stretch induces epithelial-mesenchymal transition in alveolar epithelia via hyaluronan activation of innate immunity. J Biol Chem. 2011; 286(20):17435–44. [PubMed: 21398522]
49. French DM, Kaul RJ, D'Souza AL, et al. WISP-1 is an osteoblastic regulator expressed during skeletal development and fracture repair. Am J Pathol. 2004; 165(3):855–67. [PubMed: 15331410]
50. Price RM, Tulsyan N, Dermody JJ, Schwalb M, Soteropoulos P, Castronuovo JJ Jr. Gene expression after crush injury of human saphenous vein: using microarrays to define the transcriptional profile. J Am Coll Surg. 2004; 199(3):411–8. [PubMed: 15325611]

51. Venkatachalam K, Venkatesan B, Valente AJ, et al. WISP1, a pro-mitogenic, pro-survival factor, mediates tumor necrosis factor-alpha (TNF-alpha)-stimulated cardiac fibroblast proliferation but inhibits TNF-alpha-induced cardiomyocyte death. J Biol Chem. 2009; 284(21):14414–27. [PubMed: 19339243]
52. Chong ZZ, Shang YC, Zhang L, Wang S, Maiese K. Mammalian target of rapamycin: hitting the bull's-eye for neurological disorders. Oxid Med Cell Longev. 2010; 3(6):374–91. [PubMed: 21307646]
53. Chong ZZ, Wang S, Shang YC, Maiese K. Targeting cardiovascular disease with novel SIRT1 pathways. Future Cardiol. 2012; 8(1):89–100. [PubMed: 22185448]
54. Lappas M, Permezel M. The anti-inflammatory and antioxidative effects of nicotinamide, a vitamin B(3) derivative, are elicited by FoxO3 in human gestational tissues: implications for preterm birth. The Journal of nutritional biochemistry. 2011; 22(12):1195–201. [PubMed: 21414766]
55. Maiese K, Chong ZZ, Hou J, Shang YC. New strategies for Alzheimer's disease and cognitive impairment. Oxid Med Cell Longev. 2009; 2(5):279–89. [PubMed: 20716915]
56. Maiese K, Chong ZZ, Hou J, Shang YC. Oxidative stress: Biomarkers and novel therapeutic pathways. Exp Gerontol. 2010; 45(3):217–34. [PubMed: 20064603]
57. Maiese K, Chong ZZ, Shang YC, Wang S. Translating cell survival and cell longevity into treatment strategies with SIRT1. Rom J Morphol Embryol. 2011; 52(4):1173–85. [PubMed: 22203920]
58. Poulose SM, Bielinski DF, Carrihill-Knoll K, Rabin BM, Shukitt-Hale B. Exposure to (16)O-Particle Radiation Causes Aging-Like Decrements in Rats through Increased Oxidative Stress, Inflammation and Loss of Autophagy. Radiat Res. 2011; 176(6):761–9. [PubMed: 21962006]
59. Sanz A, Soikkeli M, Portero-Otin M, et al. Expression of the yeast NADH dehydrogenase Ndi1 in Drosophila confers increased lifespan independently of dietary restriction. Proc Natl Acad Sci USA. 2010; 107(20):9105–10. [PubMed: 20435911]
60. Vendelbo MH, Nair KS. Mitochondrial longevity pathways. Biochim Biophys Acta. 2011; 1813(4):634–44. [PubMed: 21295080]
61. Yang H, Jin X, Kei Lam CW, Yan SK. Oxidative stress and diabetes mellitus. Clin Chem Lab Med. 2011; 49(11):1773–82. [PubMed: 21810068]
62. Benjamin D, Colombi M, Moroni C, Hall MN. Rapamycin passes the torch: a new generation of mTOR inhibitors. Nat Rev Drug Discov. 2011; 10(11):868–80. [PubMed: 22037041]
63. Cheng Z, White MF. Targeting Forkhead box O1 from the concept to metabolic diseases: lessons from mouse models. Antioxid Redox Signal. 2011; 14(4):649–61. [PubMed: 20615072]
64. Chong ZZ, Li F, Maiese K. Activating Akt and the brain's resources to drive cellular survival and prevent inflammatory injury. Histol Histopathol. 2005; 20(1):299–315. [PubMed: 15578447]
65. Cui W, Matsuno K, Iwata K, et al. NOX1/nicotinamide adenine dinucleotide phosphate, reduced form (NADPH) oxidase promotes proliferation of stellate cells and aggravates liver fibrosis induced by bile duct ligation. Hepatology. 2011 May 26.
66. Eliopoulos N, Zhao J, Forner K, Birman E, Young YK, Bouchentouf M. Erythropoietin Gene-enhanced Marrow Mesenchymal Stromal Cells Decrease Cisplatin-induced Kidney Injury and Improve Survival of Allogeneic Mice. Mol Ther. 2011; 19(11):2072–83. [PubMed: 21847101]
67. Hwang SK, Kim HH. The functions of mTOR in ischemic diseases. BMB Rep. 2011; 44(8):506–11. [PubMed: 21871173]
68. Koh PO. Nicotinamide attenuates the ischemic brain injury-induced decrease of Akt activation and Bad phosphorylation. Neurosci Lett. 2011; 498(2):105–9. [PubMed: 21596097]
69. Komandirov MA, Knyazeva EA, Fedorenko YP, Rudkovskii MV, Stetsurin DA, Uzdensky AB. On the role of phosphatidylinositol 3-kinase, protein kinase b/akt, and glycogen synthase kinase-3beta in photodynamic injury of crayfish neurons and glial cells. J Mol Neurosci. 2011; 45(2):229–35. [PubMed: 21318403]
70. Xie X, Li W, Lan T, et al. Berberine ameliorates hyperglycemia in alloxan-induced diabetic C57BL/6 mice through activation of Akt signaling pathway. Endocrine journal. 2011; 58(9):761–8. [PubMed: 21705841]

71. Zhou X, Wang L, Wang M, et al. Emodin-induced microglial apoptosis is associated with TRB3 induction. Immunopharmacol Immunotoxicol. 2011; 33(4):594–602. [PubMed: 21275776]
72. Li F, Chong ZZ, Maiese K. Microglial integrity is maintained by erythropoietin through integration of Akt and its substrates of glycogen synthase kinase-3beta, beta-catenin, and nuclear factor-kappaB. Curr Neurovasc Res. 2006; 3(3):187–201. [PubMed: 16918383]
73. Chong ZZ, Li F, Maiese K. Oxidative stress in the brain: Novel cellular targets that govern survival during neurodegenerative disease. Prog Neurobiol. 2005; 75(3):207–46. [PubMed: 15882775]
74. Cai W, Rudolph JL, Harrison SM, et al. An evolutionarily conserved Rit GTPase-p38 MAPK signaling pathway mediates oxidative stress resistance. Mol Biol Cell. 2011; 22(17):3231–41. [PubMed: 21737674]
75. Hsu SY, Kaipia A, Zhu L, Hsueh AJ. Interference of BAD (Bcl-xL/Bcl-2-associated death promoter)-induced apoptosis in mammalian cells by 14-3-3 isoforms and P11. Mol Endocrinol. 1997; 11(12):1858–67. [PubMed: 9369453]
76. Maiese K, Chong ZZ, Shang YC, Hou J. Therapeutic promise and principles: Metabotropic glutamate receptors. Oxid Med Cell Longev. 2008; 1(1):1–14. [PubMed: 19750024]
77. Maiese K, Chong ZZ, Hou J, Shang YC. The vitamin nicotinamide: translating nutrition into clinical care. Molecules. 2009; 14(9):3446–85. [PubMed: 19783937]
78. Putcha GV, Moulder KL, Golden JP, et al. Induction of BIM, a proapoptotic BH3-only BCL-2 family member, is critical for neuronal apoptosis. Neuron. 2001; 29(3):615–28. [PubMed: 11301022]
79. Marani M, Tenev T, Hancock D, Downward J, Lemoine NR. Identification of novel isoforms of the BH3 domain protein Bim which directly activate Bax to trigger apoptosis. Mol Cell Biol. 2002; 22(11):3577–89. [PubMed: 11997495]
80. Chong ZZ, Li F, Maiese K. Stress in the brain: novel cellular mechanisms of injury linked to Alzheimer's disease. Brain Res Brain Res Rev. 2005; 49(1):1–21. [PubMed: 15960984]
81. Canadillas S, Ortega R, Estepa JC, et al. Darbepoetin-alpha treatment enhances glomerular regenerative process in the Thy-1 glomerulonephritis model. American journal of physiology. 2010; 299(6):F1278–87. [PubMed: 20826570]
82. Chong ZZ, Lin SH, Kang JQ, Maiese K. The tyrosine phosphatase SHP2 modulates MAP kinase p38 and caspase 1 and 3 to foster neuronal survival. Cell Mol Neurobiol. 2003; 23(4–5):561–78. [PubMed: 14514016]
83. Kui L, Weiwei Z, Ling L, et al. Ghrelin inhibits apoptosis induced by high glucose and sodium palmitate in adult rat cardiomyocytes through the PI3K-Akt signaling pathway. Regul Pept. 2009; 155(1–3):62–9. [PubMed: 19289146]
84. Liang JH, Du J, Xu LD, et al. Catalpol protects primary cultured cortical neurons induced by Abeta(1-42) through a mitochondrial-dependent caspase pathway. Neurochem Int. 2009; 55(8): 741–6. [PubMed: 19631247]
85. Shang YC, Chong ZZ, Hou J, Maiese K. FoxO3a governs early microglial proliferation and employs mitochondrial depolarization with caspase 3, 8, and 9 cleavage during oxidant induced apoptosis. Curr Neurovasc Res. 2009; 6(4):223–38. [PubMed: 19807657]
86. Zhao Y, Xue T, Yang X, et al. Autophagy plays an important role in Sunitinib-mediated cell death in H9c2 cardiac muscle cells. Toxicol Appl Pharmacol. 2010; 248(1):20–7. [PubMed: 20637791]
87. Hedley BD, Allan AL, Xenocostas A. The role of erythropoietin and erythropoiesis-stimulating agents in tumor progression. Clin Cancer Res. 2011; 17(20):6373–80. [PubMed: 21750199]
88. Lombardero M, Kovacs K, Scheithauer BW. Erythropoietin: a hormone with multiple functions. Pathobiology. 2011; 78(1):41–53. [PubMed: 21474975]
89. Maiese K, Chong ZZ, Shang YC. Raves and risks for erythropoietin. Cytokine Growth Factor Rev. 2008; 19(2):145–55. [PubMed: 18299246]
90. Maiese K, Li F, Chong ZZ. Erythropoietin and cancer. JAMA. 2005; 293(15):1858–9. [PubMed: 15840858]
91. Nagai Y, Watanabe M, Ishikawa S, et al. Clinical significance of Wnt-induced secreted protein-1 (WISP-1/CCN4) in esophageal squamous cell carcinoma. Anticancer Res. 2011; 31(3):991–7. [PubMed: 21498727]

92. Hou CH, Chiang YC, Fong YC, Tang CH. WISP-1 increases MMP-2 expression and cell motility in human chondrosarcoma cells. Biochem Pharmacol. 2011; 81(11):1286–95. [PubMed: 21453685]

93. Davies SR, Davies ML, Sanders A, Parr C, Torkington J, Jiang WG. Differential expression of the CCN family member WISP-1, WISP-2 and WISP-3 in human colorectal cancer and the prognostic implications. Int J Oncol. 2010; 36(5):1129–36. [PubMed: 20372786]

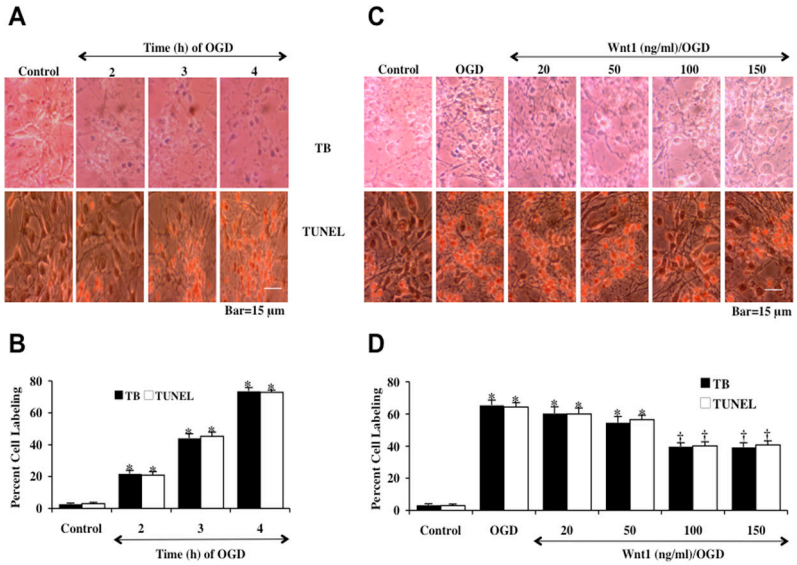

Fig. 1. Wnt1 prevents neuronal cell injury against oxygen-glucose deprivation (OGD)

(**A**) Primary hippocampal neurons were exposed to progressive durations of OGD of 2, 3 and 4 hours and cell injury was determined by trypan blue (TB) dye exclusion and TUNEL 24 hours after OGD. Representative images illustrate that OGD led to progressive neuronal cell injury with increased exposure time of OGD. In all cases, control = untreated neuronal cells. (**B**) Quantitative analysis reveals that the percent cell trypan blue staining and apoptotic DNA fragmentation was significantly increased 24 hours following OGD ($^{*}p<0.01$ *vs.* control). Each data point represents the mean and SEM from 6 experiments. (**C**) Increasing concentrations (20, 50, 100, and 150 ng/ml) of Wnt1 protein was applied to neuronal cultures 1 hour prior to a 3 hour period of OGD and cell injury was determined by trypan blue (TB) dye exclusion and TUNEL 24 hours following OGD. Wnt1 at the concentrations of 100 ng/ml and 150 ng/ml significantly reduced neuronal cell labeling of trypan blue (TB) and TUNEL 24 hours after OGD. (**D**) Quantitative analysis showed that Wnt1 (100 ng/ml and 150 ng/ml) administered 1 hour prior to OGD significantly decreased the percent cell labeling of trypan blue and percent DNA fragmentation 24 hours following OGD ($^{*}p<0.01$ *vs.* control; $^{\dagger}p < 0.01$ vs. OGD). Each data point represents the mean and SEM from 6 experiments.

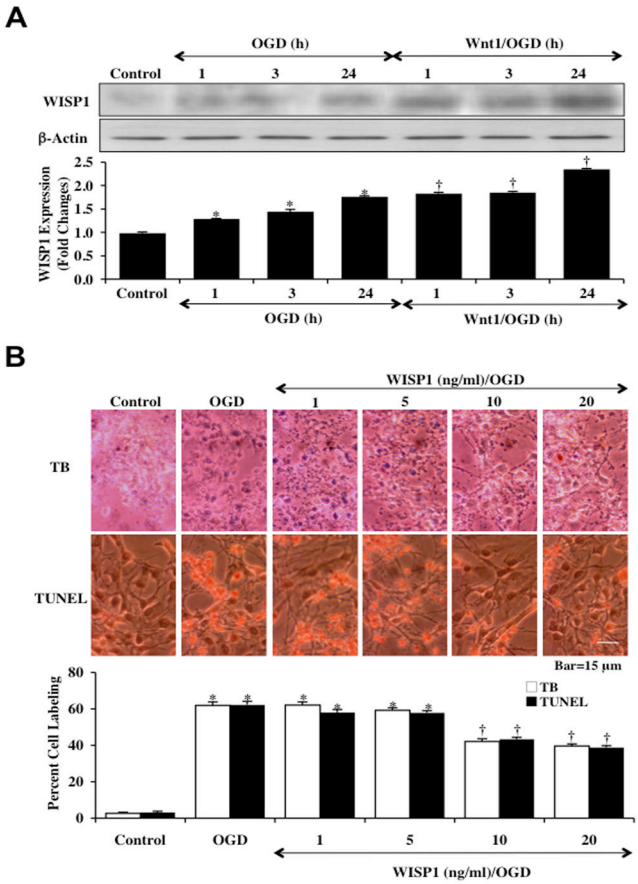

Fig. 2. Wnt1 increases and maintains expression of WISP1 with neuronal cell injury blocked by WISP1 during OGD

(**A**) Hippocampal neuronal protein extracts (50 μg/lane) were immunoblotted with anti-WISP1 at 1, 3 and 24 hours following a 3 hour period of OGD. WISP1 expression was increased at 1, 3 and 24 hours following OGD and was further significantly increased by application of Wnt1 (100 ng/ml) 1 hour prior to OGD (*p<0.01 *vs*. control; †p <0.01 *vs*. OGD of corresponding time point). Quantification of western band intensity from 3 experiments was performed using the public domain NIH Image program (http://rsb.info.nih.gov/nih-image). **(B)** Increasing concentrations (1, 5, 10, and 20 ng/ml) of WISP1 protein were applied to neuronal cultures 1 hour prior to a 3 hour period of OGD and cell injury was determined by trypan blue (TB) dye exclusion and TUNEL 24 hours following OGD. WISP1 protected neurons against OGD in a concentration dependent manner, reducing trypan blue staining and DNA fragmentation at the concentrations of 10 ng/ml and 20 ng/ml (*p<0.01 *vs*. control; †p < 0.01 vs. OGD). Each data point represents the mean and SEM from 6 experiments.

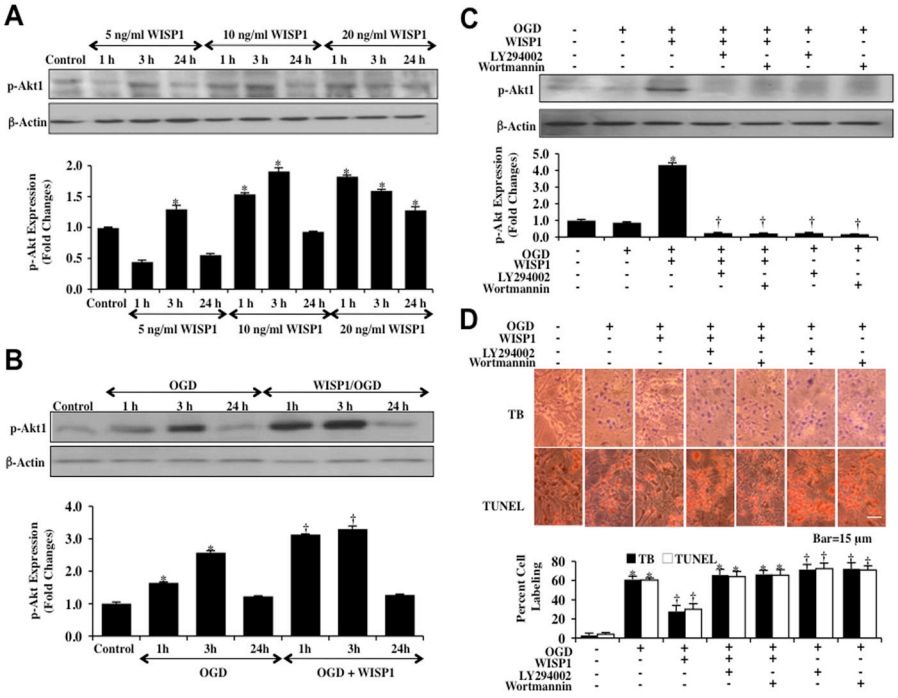

Fig. 3. WISP1 utilizes PI 3-K and Akt1 pathways to protect neurons against OGD

(**A**) Equal amounts of neuronal protein extracts (50 μg/lane) were immunoblotted at 1, 3 and 24 hours after administration of 5 ng/ml, 10 ng/ml or 20 ng/ml WISP1 with anti–phospho-Akt1 (p-Akt1, Ser^{473}) antibody. WISP1 significantly enhanced p-Akt1 expression in a concentration dependent manner (*p<0.01 vs. Control). Quantitative analysis of the western blots from 3 experiments was performed using the public domain NIH Image program (developed at the US National Institutes of Health and available on the Internet at http://rsb.info.nih.gov/nih-image/). **(B)** Equal amounts of neuronal protein extracts (50 μg/lane) were immunoblotted with p-Akt1 antibody at 1, 3 and 24 hours following a 3 hour period of OGD. The expression of p-Akt1 was increased at 1 and 3 hours following OGD exposure and was further increased by WISP1 (10 ng/ml) administration 1 hour prior to OGD (*p<0.01 vs. Control; †p <0.01 *vs*. OGD). **(C)** Application of the specific PI 3-K inhibitors wortmannin (0.5 μM) or LY294002 (10 μM) 1 hour prior to a 3 hour period of OGD abrogated WISP1 induced expression of p-Akt1 3 hours following a 3 hour period of OGD (**P*<0.01 *vs*. Control; †*P* <0.01 *vs*. WISP1/OGD). **(D)** Representative images demonstrate that OGD led to a significant increase in trypan blue staining and DNA fragmentation in neuronal cells 24 hours after OGD compared to untreated control cultures. WISP1 (10 ng/ml) application 1 hour prior to OGD significantly decreased trypan blue and TUNEL staining. Yet, combined treatment with specific PI 3-K inhibitors wortmannin (0.5 μM) or LY294002 (LY, 10 μM) abrogated the ability of WISP1 to reduce trypan blue staining and DNA fragmentation. Quantitative results illustrate that WISP1 (10 ng/ml) application significantly decreased percent trypan blue uptake and DNA fragmentation 24 hours after OGD when compared to OGD. Combined treatment with specific PI 3-K inhibitors wortmannin or LY294002 significantly reduced the efficacy of WISP1, resulting in an increase in percent trypan blue uptake and DNA fragmentation (*p <0.01 *vs*. untreated control; †*P* <0.01 *vs*. OGD). Each data point represents the mean and SEM from 6 experiments.

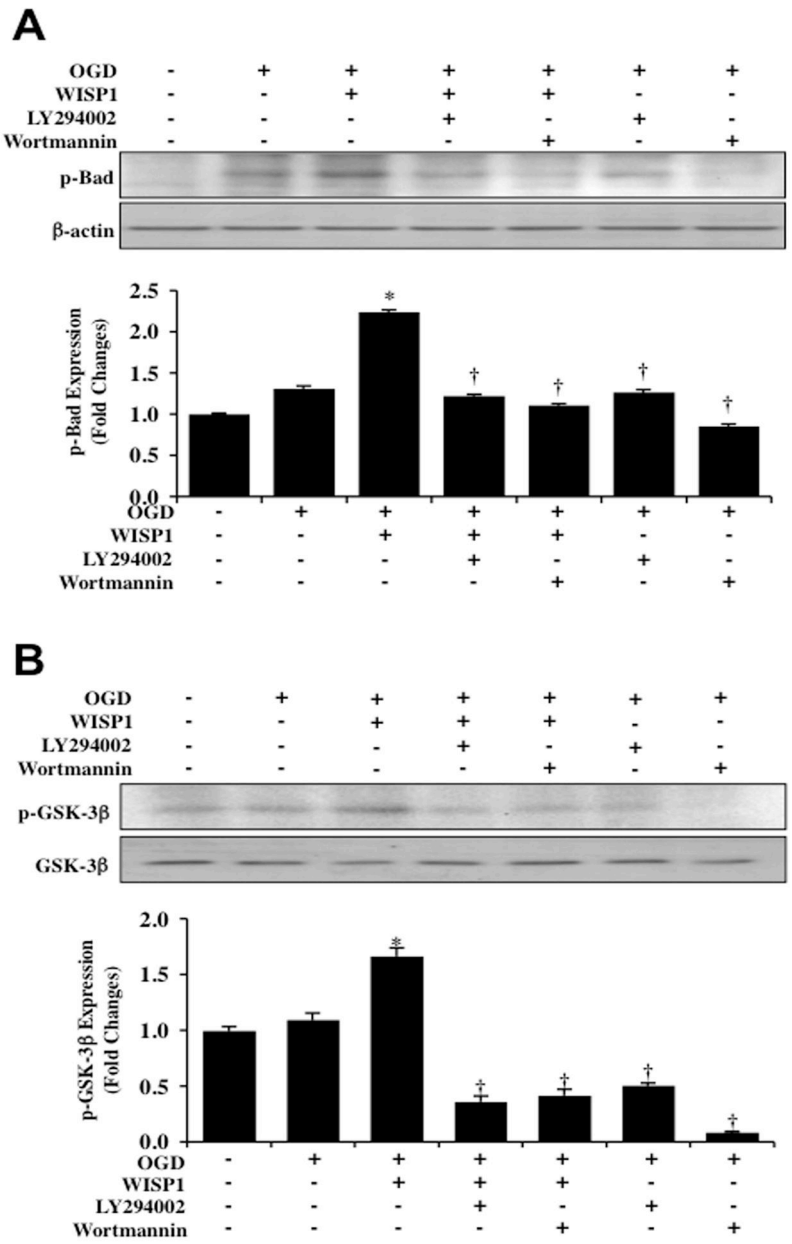

Fig. 4. WISP1 promotes Bad and GSK-3β phosphorylation through PI 3-K and Akt1 pathways during OGD

(**A**) Equal amounts of neuronal protein extracts (50 μg/lane) were immunoblotted with antibody against phosphorylated Bad (p-Bad) 3 hour following a 3 hour period of OGD. Application of WISP1 (10 ng/ml) 1 hour prior to OGD significantly increased p-Bad expression compared with OGD treated alone. Combined application of the specific PI 3-K inhibitors wortmannin (0.5 μM) or LY294002 (10 μM) prevented WISP1 phosphorylation of Bad 3 hours following OGD (*p<0.01 *vs*. OGD; †*P* <0.01 *vs*. WISP1/OGD). **(B)** Equal amounts of neuronal protein extracts (50 μg/lane) were immunoblotted with antibody against phosphorylated GSK-3β (p-GSK-3β) 3 hours following a 3 hour period of OGD. WISP1 (10 ng/ml) administered 1 hour prior to OGD significantly increased p-GSK-3β expression compared with OGD alone. Combined application of wortmannin (0.5 μM) or LY294002 (10 μM) prevented WISP1 phosphorylation of GSK-3β following OGD (*p<0.01

vs. OGD; †*P* <0.01 *vs*. WISP1/OGD). In A and B, quantitative analysis of western blots from 3 experiments was performed using the public domain NIH Image program (developed at the US National Institutes of Health and available on the Internet at http://rsb.info.nih.gov/nih-image/).

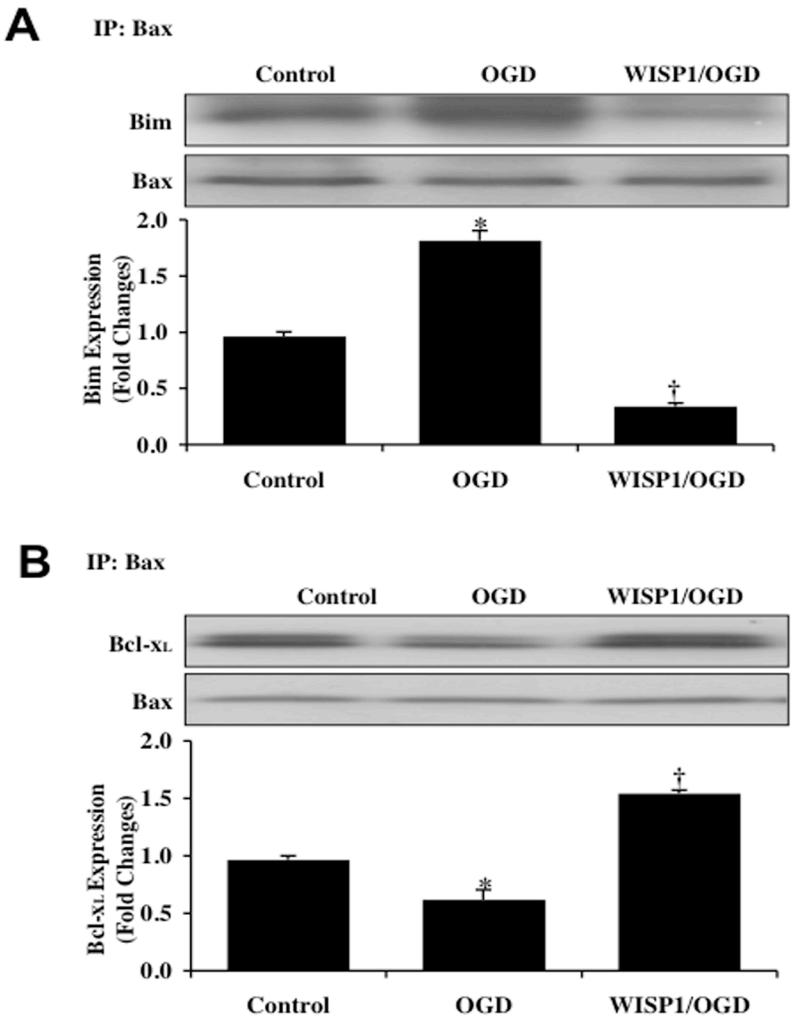

Fig. 5. WISP1 dissociates Bim from Bax and increases the binding of Bcl-x_L to Bax during OGD

Neuronal cell protein extracts were immunoprecipited by using Bax antibody 3 hours following a 3 hour period of OGD and immunoprecipitation for Bim (**A**) and Bcl-x_L (**B**) binding activity to Bax was performed. OGD resulted in an increase in the binding ability of Bim to Bax, but decreased association of Bcl-x_L with Bax. Application of WISP1 (10 ng/ml) 1 hour prior to OGD dissociated Bim from Bax and increased the binding of Bcl-x_L to Bax during OGD ($^{*}p < 0.01$ *vs*. untreated control; $^{\dagger}p < 0.01$ *vs*. OGD). Quantification of western band intensity was performed using the public domain NIH Image program (http://rsb.info.nih.gov/nih-image). Each data point represents the mean and SEM from 3 experiments.

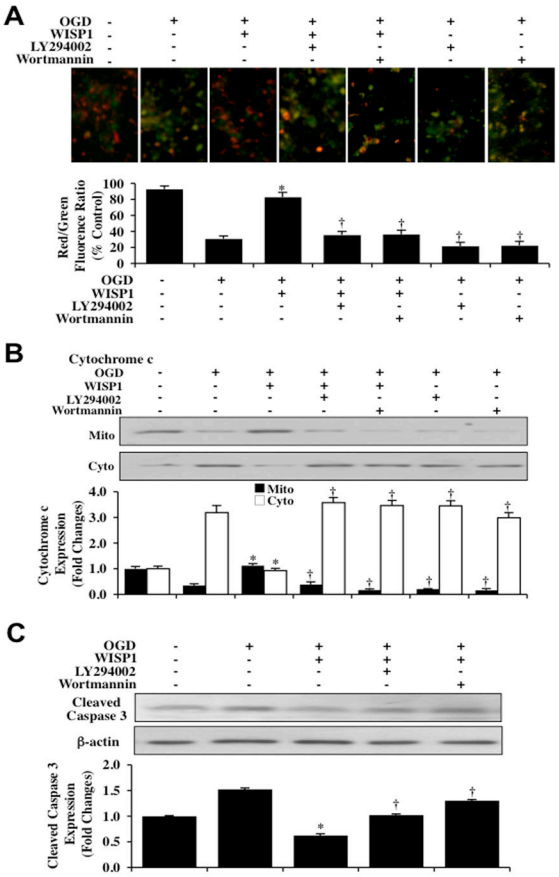

Fig. 6. WISP1 maintains mitochondrial membrane polarization while preventing cytochrome c release and the activation of caspase 3 through PI 3-K and Akt1 pathways during OGD

(**A**) Representative images and quantitative results from JC-1 staining reveal that OGD exposure produces a significant decrease in the red/green fluorescence intensity ratio of mitochondria within 3 hours when compared with untreated control cultures, demonstrating that mitochondrial membrane depolarization occurs 3 hours following OGD. WISP1 (10 ng/ml) 1 hour pretreatment significantly increased the red/green fluorescence intensity of mitochondria in neurons, demonstrating that mitochondrial membrane potential was restored. In contrast, inhibition of PI 3-K with wortmannin (0.5 μM) or LY294002 (10 μM) abrogated the ability of WISP1 to increase the mitochondrial membrane potential during OGD. The relative ratio of red/green fluorescent intensity of mitochondrial staining was measured in 3 independent experiments with analysis performed using the public domain NIH Image program (http://rsb.info.nih.gov/nih-image) (*$p<0.01$ *vs*. OGD; †$p<0.01$ *vs*. WISP1/OGD). (**B**) Equal amounts of mitochondrial (mito) or cytosol (cyto) protein extracts (20 μg/lane) were immunoblotted with cytochrome c antibody demonstrating that WISP1 significantly prevented cytochrome c release from mitochondria 3 hours after a 3 hour period of OGD. The specific PI 3-K inhibitors wortmannin (0.5 μM) or LY294002 (10 μM) abrogated the ability of WISP1 to prevent cytochrome c release during OGD (*$p<0.01$ *vs*. OGD; †$p<0.01$ *vs*. WISP1/OGD). Quantification of the western band intensity was performed using the public domain NIH Image program (http://rsb.info.nih.gov/nihimage). (**C**) Neuronal cell protein extracts (50 μg/lane) were immunoblotted with cleaved caspase 3 (active) antibody 3 hours after a 3 hour period of OGD. OGD significantly increased cleaved caspase 3 expression. In contrast, WISP1 (10 ng/ml) administered 1 hour prior to OGD markedly prevented the expression of cleaved caspase 3 during OGD. The specific PI 3-K

inhibitors wortmannin (0.5 μM) or LY294002 (10 μM) blocked the ability of WISP1 to prevent caspase 3 activation (*$p<0.01$ *vs*. OGD; $^{\dagger}p<0.01$ *vs*. WISP1/OGD). Quantification of western band intensity from 3 experiments was performed using the public domain NIH Image program (http://rsb.info.nih.gov/nih-image).